

Airborne hyperspectral detection of microbial mat pigmentation in Rangiroa atoll (French Polynesia)

*Serge Andréfouët*¹

University of South Florida, Institute for Marine Remote Sensing, College of Marine Science, 140 7th Avenue South, St. Petersburg, Florida 33701

Claude Payri

Université de la Polynésie Française, Laboratoire d'Ecologie Marine, BP 6570 Faaa-Aéroport, Tahiti, French Polynesia

Eric J. Hochberg

University of Hawaii, Department of Oceanography, 1000 Pope Road, Honolulu, Hawaii 96822

Lydie Mao Che

Université de la Polynésie Française, Laboratoire d'Ecologie Marine, BP 6570 Faaa-Aéroport, Tahiti, French Polynesia

Marlin J. Atkinson

University of Hawaii, Hawaii Institute of Marine Biology, P.O. Box 1346, Kaneohe, Hawaii 96744

Abstract

The pigmentation of a cyanobacterial mat located in Rangiroa atoll (French Polynesia) was characterized using low-altitude (500 m) Compact Airborne Spectrometer Imager hyperspectral measurements. Peaks in second and fourth derivatives of the reflective absorbance can be explained by chlorophyll and carotenoid pigments, which were independently identified by high-pressure liquid chromatography. Phycobilin pigments were also detected from airborne measurements. The study confirms the extensibility of derivative spectroscopy from *in vivo* to high-resolution remote sensing measurements for biology and geochemistry investigations in marine communities.

Microbial mats are peculiar microecosystems encountered worldwide in various coastal environments. They are abundant in many atoll lagoons of the Pacific Ocean, particularly along atoll rims in the Tuamotu Archipelago (French Polynesia) at the lagoon/land interface and in large ponds inside islets (Défarge et al. 1994a). In Polynesian islands, these microbial mats are called “kopara.” They are gelatinous deposits a few tens of centimeters thick, typically with a vivid orange to red color that can shift to dark green or black with local development of the cyanobacterium *Scytonema*. Kopara mats persist under contrasting environmental situations,

from submergence in shallow pools to completely dry, presenting desiccated polygonal patterns. In environments protected from wave flushing and from human and animal perturbations, kopara are generally vertically laminated with oxygenic phototrophic prokaryotes (cyanobacteria) in the upper layers and anoxygenic phototrophic and anaerobic heterotrophic bacteria in the deeper horizons (Défarge et al. 1994b; Rougeaux et al. 2001). The complex vertical organization of the microorganisms results from gradients of light, oxygen, and sulfide. Previous studies have presented the biogeochemistry of these microecosystems, where carbonate precipitation in the form of modern stromatolites occurs (Défarge et al. 1994a,b).

As part of a research program on the ecology and biotechnology of these mats, kopara have been inventoried on Rangiroa atoll in 1998 (15°14'S, 147°60'W, French Polynesia; Fig. 1) with multispectral remote sensing data (Andréfouët et al. in press). The image-based inventory and subsequent *in situ* survey enabled the reconnaissance of a few highly stratified kopara mats that later confirmed their biotechnological potential (Rougeaux et al. 2001). Preliminary results obtained from two Rangiroa kopara mats show that their upper layers are a source of promising exopolysaccharides (EPSs) for biotechnological applications. High levels of EPSs in the first 3 cm of the mats are due to high concentrations of cyanobacteria (Rougeaux et al. 2001). This is reflected in the pigmentation of the different kopara layers,

¹ Corresponding author (serge@seas.marine.usf.edu).

Acknowledgments

CASI images were collected during the expedition of the vessel *Golden Shadow* to French Polynesia and were made available thanks to the extraordinary generosity of her owner, HRH Prince Khaled bin Sultan bin Abdulaziz of Saudi Arabia, via Herb Ripley (Hyperspectral Data Int.). Jean Jaubert and John R. M. Chisholm, Observatoire Océanographique Européen, Monaco, coordinated the CASI flights. Laura Roy (HDI) preprocessed the CASI data.

This project was partly funded by NASA awards NAG5-7513 and NAG5-5276 and NOAA award NA07-OA0571 to M.J.A. The Ministry of Health and Research of the Government of French Polynesia supported this research with a grant to C.P.

HIMB contribution 1132 and SOEST contribution 6015. The Office of Naval Research, Environmental Optics Program, is acknowledged for supporting this publication.

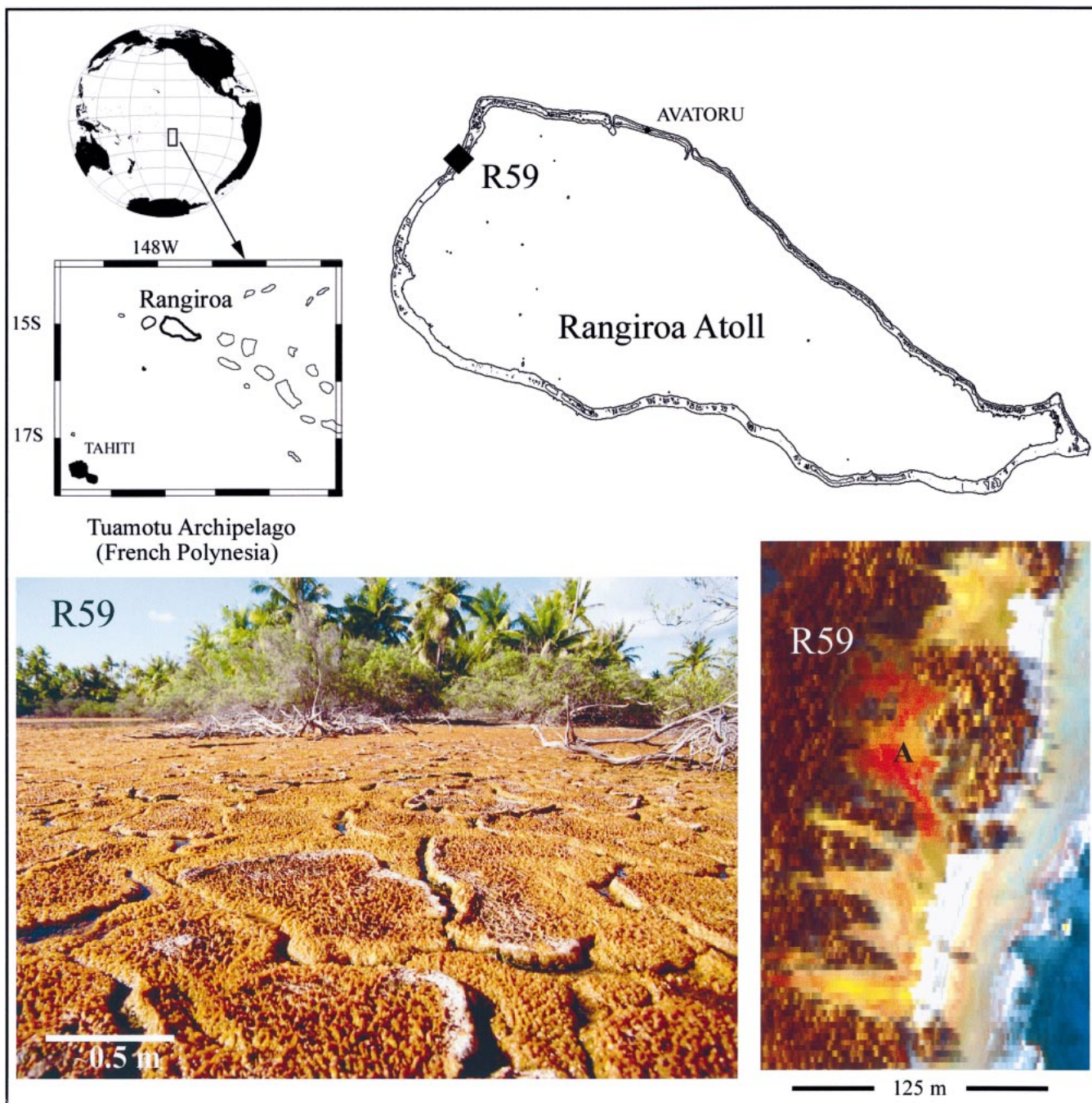


Fig. 1. Map of Rangiroa atoll and location of the R59 kopara mat. CASI spectra and the sample for pigment analysis came from the region marked A, the purest part of the mat. The structure and aspect of the surface is revealed in the photograph on the bottom left. The image on the right is an RGB color composite obtained with CASI bands R = 700, G = 571, and B = 460 nm.

with decreasing cyanobacterial pigments at depth (Mao Che et al. 2001). Pigmentation of the different layers has been characterized and quantified using high-pressure liquid chromatography (HPLC, Mao Che et al. 2001). For the kopara mat labeled R59 (Fig. 1), the upper layer (0–0.5 cm) was vivid orange and was dominated by the cyanobacteria *Schizothrix* sp. and *Phormidium* spp., with a lesser presence of *Chloroflexus*-like bacteria. HPLC analysis of this layer indicated high concentrations of chlorophyll *a* (Chl *a*, 40 μg

g^{-1} dry weight), beta-carotene (20 μg g^{-1} dry weight), and myxoxanthophyll (15 μg g^{-1} dry weight); much smaller (<5 μg g^{-1} dry weight) concentrations of bacterio-Chl *a*, canthaxanthin, echinenone, and zeaxanthin; and traces (1 μg g^{-1} dry weight) of pheophytin, gamma-carotenes, and other various minor carotenoids (Mao Che et al. 2001).

Considering the remarkable characteristics of kopara and their biotechnological potential (EPSs), our goal is to determine whether the pigmentation of the surface of the mats

can be detected by remote sensing techniques. In this study, we compare airborne spectroscopy of kopara to pigment analysis of the upper layers of these bacterial mats.

Materials and methods

We used a Compact Airborne Spectrometer Imager (CASI) hyperspectral image of the kopara mat R59 (Fig. 1), acquired at low altitude (500 m) in May 1998. The hypercube is made of 27 spectral bands evenly distributed between 400 and 700 nm. Because the duration of the measurement lengthens pixels along the flight track, the spatial resolution achieved was 1×5.5 m. CASI is calibrated by the ITRES company on an annual basis. The accuracy of radiometric calibration of the CASI is estimated to be $\pm 2\%$, from 470 to 700 nm, and $\pm 5\%$ between 400 and 470 nm (Babey and Soffer 1992). Atmospheric conditions at the time of the survey were estimated using the software 6S (Vermotte et al. 1997), assuming clear oceanic atmosphere. CASI total radiance L_t and CASI atmospherically corrected radiance L_w were normalized by the downwelling irradiance E_d to provide measurements consistent with remote sensing reflectance (R_{rs} , sr^{-1}). E_d came from the spectral solar irradiance model described in Gregg and Carder (1990) after spectral binning to match CASI wavebands. Reflectance spectra came from 13 pixels located in the purest part of the mat (Fig. 1) without mixing by vegetation, sand, or overlaying shallow waters. Spectra were transformed into reflective absorbance (A) (Talsky 1994) with the following equation.

$$A = \log_{10}(1/R_{rs})$$

The CASI spectra were then interpolated to 1 nm resolution and smoothed three times using the Savitsky–Golay least-square method (Savitsky and Golay 1964). Absorption features were identified by computing second and fourth derivatives with respect to wavelength. The derivatives were computed using a one-pass 21-point convolution window. An abundant literature comments on the effects of smoothing using Savitsky–Golay techniques (e.g., Butler and Hopkins 1970; Talsky 1994; Hochberg and Atkinson 2000). It has been demonstrated that it creates a negligible effect on amplitude and location of derivative peaks. Our own tests suggest that, generally, the shift is 1 nm, with a maximum of 3 nm.

Derivative analysis provides information on the concavity and convexity of the spectrum shape. Here, positive peaks on the second and fourth derivatives (the sign of the second derivative curve has been reversed) represent absorption features, potentially due to one or more pigments. Compared to the gross features readily visible in zero-order absorption spectra, derivatives resolve small secondary peaks and could help to determine the individual pigments present in the regions of overlapping absorption domain (e.g., the 400–500-nm region for the carotenoids). Derivative analysis of *in vivo* absorption spectra has been employed to characterize the pigmentation of fleshy and calcifying algae (e.g., Smith and Alberte 1994; Payri et al. 2001). Bidigare et al. (1989) and, more recently, Aguirre-Gomez et al. (2001) also used derivatives to identify pigments in oceanic waters. Aguirre-Gomez et al. (2001) showed that second derivatives might miss

some peaks that are visible on fourth derivatives if the individual pigment absorption curves are gaussian, as opposed to lorentzian-shaped. Thus, we compute both second and fourth derivatives. From a remote sensing standpoint, the technique has been applied to a cyanobacterial pond environment near San Francisco using high-altitude airborne visible infrared imaging spectrometer (AVIRIS) hyperspectral imagery (Richardson et al. 1994). Despite processing only at-sensor total radiance and despite the possible interference by atmospheric absorption during high-altitude flights, some fourth derivatives peaks were attributed to very specific pigments (e.g., myxoxanthophyll), which were independently identified by HPLC.

To achieve our goal, we compared kopara HPLC pigment composition data with pigments identified through derivative analyses of spectral signatures extracted from airborne hyperspectral imagery. To be cautious, however, we first performed a test to determine whether pigments are detectable in derivatives of absorption spectra obtained through spectrophotometric analysis of kopara samples.

Samples collected in October 1998 from the first 0.5 cm of the mat were lyophilized and extracted in methanol/acetone (2:2, then 1:3, then 0:4, vol:vol). Absorption measurements were performed using a Kontron–Uvikon (model 860) at 0.5 nm resolution. Pigments were then identified by comparing the second and fourth derivative peaks of the total absorption spectra with individual pigment absorption peaks. Hypsochromic (decrease in wavelength) shifts can occur when pigments are isolated in solvent (Smith and Alberte 1994); hence, an adequate extraction protocol must be considered when consulting databases of individual pigment absorptions (Rowan 1989; Jeffrey et al. 1997).

Results and discussion

Absorption spectra measured directly from kopara samples show prominent shoulders near 422, 448, 478, and 659 nm (Fig. 2). More subtle variations are highlighted by second derivatives at 508 nm and between 550 and 625 nm. The second derivative peaks are explained by the presence of Chl *a* (422, 659 nm), myxoxanthophyll (508 nm), and combinations of various carotenoids (422, 448, and 478 nm) (Jeffrey et al. 1997). Fourth derivatives of the absorption spectrum still clearly resolve the 422, 448, 480, 508, and 657 peaks but also resolve minor peaks (541, 559, 578, 592, 608, and 628 nm) between 525 and 630 nm (Fig. 2). These can be interpreted as the combination of the signatures of pheophytin (559 and 608 nm) and the three minor absorptions peaks (541, 578, 608) of Chl *a* in this range (Jeffrey et al. 1997). These observations are consistent with HPLC data. The expected pigments are identified in the derivatives, and the most significant peaks are obtained for pigments with higher concentrations. This test validates pigment identification using derivative analysis in kopara; the next step is to apply the technique to airborne measurements.

All CASI reflective absorbance spectra exhibit prominent bumps at 630 and 677 nm and a shoulder at 520–530 nm (Fig. 3). The characteristic triple-peak feature visible on the kopara absorption between 410 and 490 nm (Fig. 2) is clear-

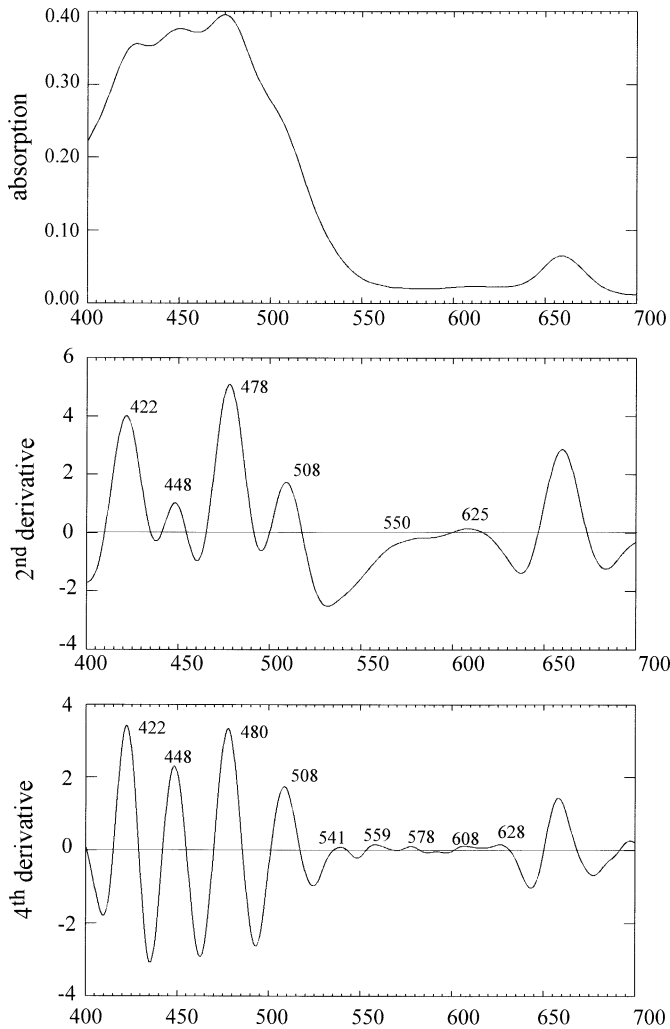


Fig. 2. Absorption spectrum of the kopara surface and second and fourth derivatives.

ly visible on most of the individual spectra (Fig. 3), although the positions of these peaks vary from one pixel to another. As a result, the average spectrum is smoother (Fig. 4). The maximum contribution of the atmospheric radiance to the total radiance was $\sim 25\%$ in the range 400–415 nm, $<15\text{--}10\%$ between 415 and 500 nm, and $<1\%$ above 500 nm. However, histograms of second derivatives of CASI spectra (Fig. 3), with or without atmospheric correction, are similar, thus reflecting the minor influence of the atmosphere in derivatives computations. The histogram of second derivative peaks for CASI measurements clearly shows absorption modes centered at 482, 508, 533, 570, 592, 627, and 680 nm (Fig. 3). More diffuse signatures exist between 400 and 470 nm, where pooling all the pixels identifies two broad modes at 418 and 450 nm, but local peaks exist at 415, 430, 440, 450, and 460 nm for different clusters of pixels. The fourth derivatives (Fig. 4) do not add significant patterns compared to the second derivatives (Fig. 2). This diffuse signature in the lowest range of the spectrum can be ascribed to overlapping carotenoid peaks (Richardson et al. 1994), to interferences at the surface of the mat because of presence

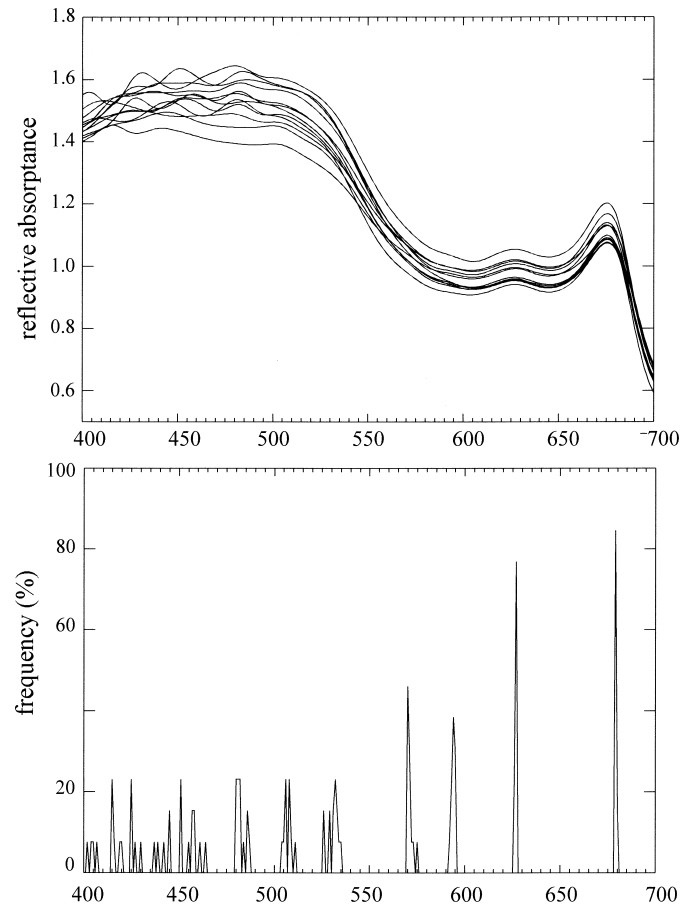


Fig. 3. Airborne reflective absorbance spectra for 13 pixels, located in the most homogeneous part of the R59 mat, and histogram (%) of the peaks in second derivatives.

of sand or other organic materials (e.g., vegetation debris), to the poorest calibration of CASI in the blue bands (Babey and Soffer 1992), or to the possible shift of peaks located at the boundary of the CASI initial bands. This last possibility, however, was not observed for higher wavelengths. Chl *a* is unambiguously detected by its red peak at 680 nm. The 428-nm peak, visible on the average of the fourth derivatives, can be attributed to the expected in vivo Soret peak of chlorophyll (Fig. 4) and to various carotenoids that modulate the signal below 500 nm. The carotenoid myxoxanthophyll, only found in cyanophytes and abundant in the kopara, is also clearly detected at 508 nm (Richardson et al. 1994). The prominent peaks at 534, 570, 594, and 628 nm, which were absent on the absorption spectra performed after solvent extraction, are explained by phycobilin pigments. Indeed, similar combinations of peaks at 539/569 and 595/632 nm were observed for red algae by Beach et al. (1997) on fourth derivatives of in vivo absorption. They were attributed to R-phycoerythrin (R-PE) and R-phycoerythrin (R-PC), respectively. These patterns are also consistent with in vivo phycobilin signatures of the coralline red alga *Hydrolithon onkodes* (Payri et al. 2001).

This experiment confirmed the extensibility of derivative spectroscopy from in vivo to remote sensing studies. We

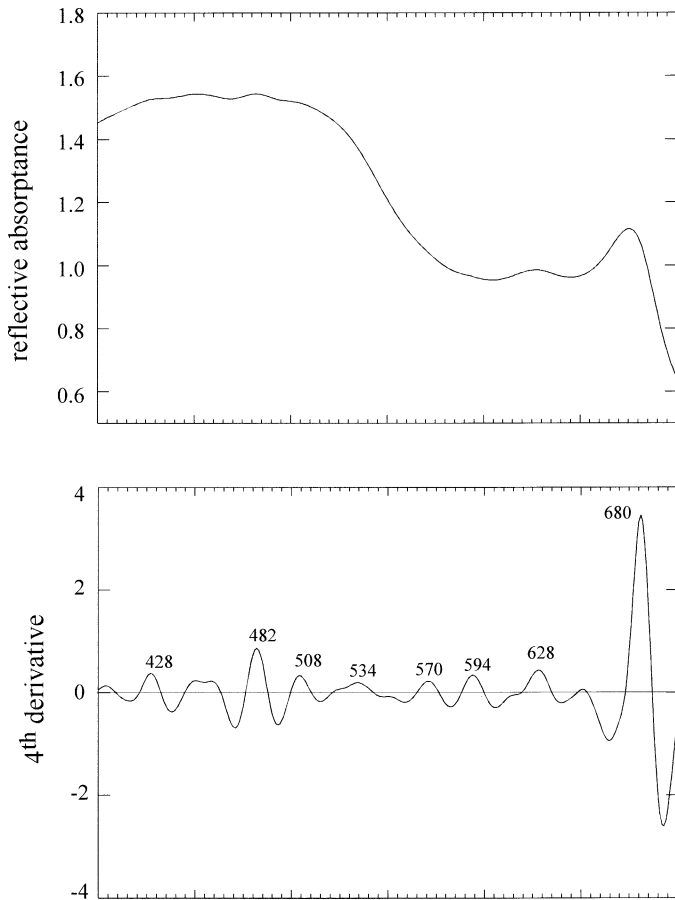


Fig. 4. The average CASI absorbance spectrum and its fourth derivative. Compare with Fig.2.

have confirmed that it is possible to perform low-altitude airborne assessment of pigmentation in homogeneous substrates. Importantly, this result was achieved without the need to spatially average pixels to improve the signal to noise ratio. Therefore, this type of analysis can be performed at small scales over small communities covering few square meters. We cannot construct a quantitative relation between reflectance/absorbance and pigment concentration (as in Myers et al. 1999) because we were unable to apply our approach to a wide range of kopara mats presenting different pigment concentrations. For instance, another mat in Rangiroa atoll has one order of magnitude more chlorophyll than R59 (Mao Che et al. 2001), but unfortunately, no CASI data were acquired on this mat. Nevertheless, our results represent an encouraging step toward the development of remote sensing bio-optical algorithms. Here, we focused on homogeneous microbial mats, but a similar approach could be used for shallow coral reef flats where heterogeneous covers of corals, fleshy algae, or encrusting coralline algae occur.

References

- AGUIRRE-GOMEZ, R., A. R. WEEKS, AND S. R. BOXALL. 2001. The identification of phytoplankton pigments from absorption spectra. *Int. J. Remote Sens.* **2**: 315–338.
- ANDRÉFOUËT, S., E. J. HOCHBERG, C. E. PAYRI, M. J. ATKINSON, F. E. MULLER-KARGER, AND H. RIPLEY. In press. Multi-scale remote sensing of microbial mats in atoll environments. *Int. J. Remote Sens.*
- BABEY, S. K., AND R. J. SOFFER. 1992. Radiometric calibration of the compact airborne spectrographic imager (CASI). *Can. J. Remote Sens.* **18**: 233–242.
- BEACH, K. S., H. B. BERGEAS, N. J. NISHIMURA, AND C. M. SMITH. 1997. In vivo absorbance spectra and the ecophysiology of reef macroalgae. *Coral Reefs* **16**: 21–28.
- BIDIGARE, R. R., J. H. MORROW, AND D. A. KIEFER. 1989. Derivative analysis of spectral absorption by photosynthetic pigments in the western Sargasso Sea. *J. Mar. Res.* **47**: 323–341.
- BUTLER, W. L., AND D. W. HOPKINS. 1970. Higher derivative analysis of complex absorption spectra. *Photochem. Photobiol.* **12**: 439–450.
- DÉFARGE, C., J. TRICHET, AND A. COUTÉ. 1994a. On the appearance of the cyanobacterial calcification in modern stromatolites. *Sediment. Geol.* **94**: 11–19.
- , ———, A. MAURIN, AND M. HUCHER. 1994b. Kopara in Polynesian atolls: Early stages of formation of calcareous stromatolites. *Sediment. Geol.* **89**: 9–23.
- GREGG, W. W., AND K. L. CARDER. 1990. A simple spectral solar irradiance model for cloudless maritime atmospheres. *Limnol. Oceanogr.* **35**: 1657–1675.
- HOCHBERG, E. J., AND M. J. ATKINSON. 2000. Spectral discrimination of coral reef benthic communities. *Coral Reefs* **19**: 164–171.
- JEFFREY, S. W., R. F. C. MANTOURA, AND S. W. WRIGHT. 1997. *Phytoplankton pigments in oceanography*. UNESCO.
- MAO CHE, L., AND OTHERS. 2001. Physical, chemical and microbiological characteristics of microbial mats (Kopara) in South Pacific atolls of French Polynesia. *Can. J. Microbiol.* **47**: 994–1012.
- MYERS, M. R., J. T. HARDY, C. H. MAZEL, AND P. DUSTAN. 1999. Optical spectra and pigmentation of Caribbean reef corals and macroalgae. *Coral Reefs* **18**: 179–186.
- PAYRI, C. E., S. MARITORENA, C. BIZEAU, AND M. RODIÈRE. 2001. Photoacclimation in the tropical coralline alga *Hydrolithon onkodes* (Rhodophyta, Corallinaceae) from a French Polynesian reef. *J. Phycol.* **37**: 223–234.
- RICHARDSON, L. L., D. BUISSON, C. J. LIU, AND V. AMBROSIA. 1994. The detection of algal photosynthetic accessory pigments using airborne visible-infrared imaging spectrometer (AVIRIS) spectral data. *Mar. Technol. Soc. J.* **28**: 10–21.
- ROUGEAUX, H., M. GUEZENNEC, L. MAO CHE, C. E. PAYRI, E. DESLANDES, AND J. GUEZENNEC. 2001. Microbial communities and exopolysaccharides from Polynesian mats. *Mar. Biotechnol.* **3**: 181–187.
- ROWAN, K. S. 1989. *Photosynthetic pigments of algae*. Cambridge Univ. Press.
- SAVITSKY, A., AND M. J. E. GOLAY. 1964. Smoothing and differentiation of data by simplified least square procedure. *Anal. Chem.* **36**: 1627–1639.
- SMITH, C. M., AND R. S. ALBERTE. 1994. Characterization of in vivo absorption features of chlorophyte, phaeophyte and rhodophyte algal species. *Mar. Biol.* **118**: 511–521.
- TALSKY, G. 1994. *Derivative spectrophotometry: Low and high order*. Weinheim.
- VERMOTE, E. F., D. TANRÉ, J. L. DEUZE, M. HERMAN, AND J. J. MORCRETTE. 1997. Second simulation of the satellite signal in the solar spectrum, 6S: An overview. *IEEE Trans. Geosci. Remote Sens.* **35**: 675–686.

Received: 1 October 2001

Accepted: 31 May 2002

Amended: 19 July 2002